Int. J. Multiphase Flow Vol. 15, No. 2, pp. 227–239, 1989
Printed in Great Britain.

0301-9322/89 $3.00 + 0.00

THE INFLUENCE OF FLOW OBSTRUCTIONS ON THE FLOODING PHENOMENON IN VERTICAL CHANNELS

G. P. CELATA, N. CUMO, G. E. FARELLO and T. SETARO
ENEA Casaccia TERM/ISP Heat Transfer Laboratory, Via Anguillarese 301, 00060 Rome, Italy

(*Received* 19 *April* 1988; *in revised form* 17 *October* 1988)

Abstract—The flooding phenomenon limits the stability of liquid–gas countercurrent flow inside a channel. As is known, this entrainment effect can completely prevent the liquid from falling down. A local flow channel cross section reduction, e.g. due to the presence of an obstruction, will affect the flooding parameters, depending on the obstruction location and on the obstruction flow cross section. The present work deals with air–water experiments performed with a transparent circular duct test section, inside which it is possible to insert orifices of different diameters, to test the effect of obstructions on the flooding phenomenon. Predictions obtained by using correlations available in the literature are compared with the experimental data and a method to evaluate the influence of such obstructions is proposed.

Key Words: flooding, obstruction, countercurrent, perforated plates, experimental, air–water, onset of flooding, zero penetration, partial delivery

1. INTRODUCTION

The so-called "countercurrent flow limitation" or "flooding" phenomenon is due to the interaction between an upward-flowing gas inside a channel, and a countercurrent falling liquid along the wall. Flooding was reviewed previously by Bankoff & Lee (1983, 1986).

The relevance of the phenomenon is known in both the chemical (distillation and absorption columns) and nuclear (emergency cooling and accident situations) industries.

The aim of the present work is to evaluate the effect of obstructions placed inside the test channel with reference to the phenomena investigated in free channel conditions. The test channel represents a simple version of an important industrial item, namely rod bundles with spacer grids.

Experimental results and a comparison with predictions from correlations available in the literature are reported. A modification of the most widely used Wallis correlation is proposed to take into account the effect of the obstructions, and obtain a good prediction of the experimental data.

2. THE EXPERIMENTAL SETUP

The experimental tests were carried out with an air–water loop named FLEX, sketched in figure 1. The test section is made of plexiglass, in order to obtain visual information and to verify the correct carrying out of the tests. The full vertical test section length is 500 mm. The distance between the water injection point and the obstruction (orifice) is 300 mm (i.e. the part of the test section above the obstruction, L_1), whilst the distance between the orifice and the gas inlet point (i.e. the part of the test section below the obstruction, L_2) is 200 mm. The inner test channel diameter is 20 mm. The obstruction consists of a disk with a central sharp-edge circular hole. The disk thickness is equal to 1/10 of the hole diameter (see figure 1).

Instrumentation consists of thermocouples and pressure transducers at the inlet of the test section for measuring the thermodynamic gas conditions, and of differential pressure transducers across the obstruction and over the test section length for pressure drop measurements.

Demineralized water is supplied from the top of the test section through a circular weir; its flow rate is measured using turbine flowmeters. Air is supplied from the bottom of the test section; its flow rate is measured using a calibrated sonic disk.

Before entering the test section, air flows through a vertical 7° convergent duct connected to the test channel. It enables the gas to get through the test channel with an already developed and steady

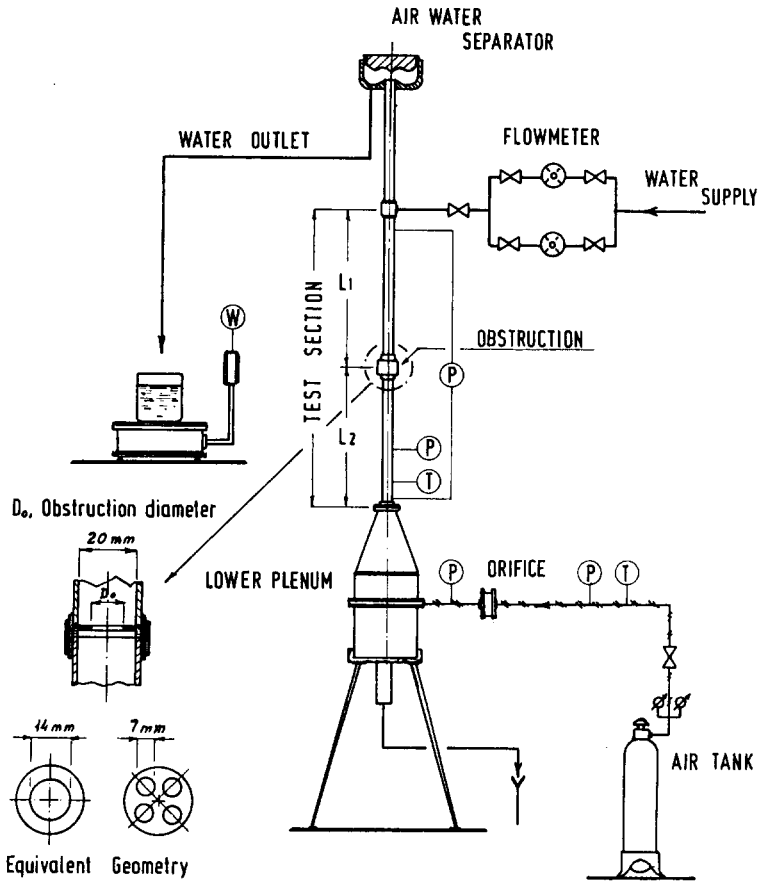

Figure 1. Schematic of the test loop.

velocity profile. Entrained water is separated from the gas–water mixture in a high-efficiency air–water separator, placed at the top end of the test channel (just above the water injection point), and collected in a small tank. The average value of the entrained water mass flow rate is obtained by weighing the water collected during the test. In order to get the minimum scattering in data measurements, the collecting time was always >2 min.

3. EXPERIMENTAL RESULTS

The test matrix

The experimental program consisted of 700 tests. The range of variation of the parameters was as follows:

• liquid mass flow rate (g/s)	5, 6.7, 8.3, 12, 17, 20, 25
• obstruction diameter (mm)	12, 14–19
• gas velocity (m/s)	0.5–15
• reference free channel diameter (mm)	20.0
• fraction of the obstruction area occupied by the hole (perforation ratio), γ	0.36, 0.49, 0.56, 0.64, 0.72, 0.81, 0.90, 1.00

Additional tests were carried out with a 16.2 mm test section, same L/D, and with values of γ equal to 0.56 and 0.72. The purpose of these tests was to provide further data with the same values of γ but with different geometries.

As far as the obstruction with a flow diameter of 14 mm is concerned, in addition to the simple centered geometry, a complex equivalent geometry (in terms of area) was also employed. The complex geometry had the same flow area, but four symmetric holes, with a flow diameter of 7 mm each (see figure 1).

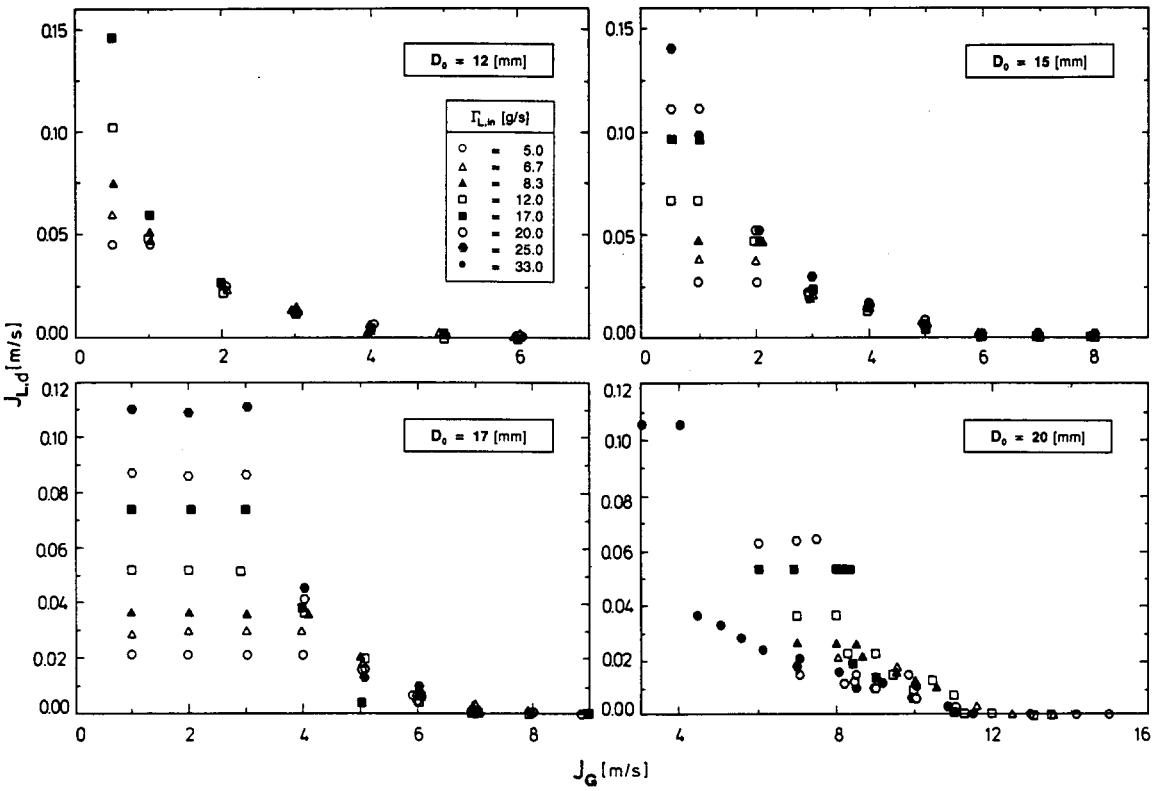

Figure 2. Experimental results: delivered liquid superficial velocity vs gas superficial velocity.

Basic definitions

The point at which the liquid falling film begins to be entrained by the upward-flowing gas is called the "onset of flooding". It is characterized by a well-defined (critical) value of the gas velocity. Such a condition is also characterized by a sudden increase in the pressure drop both across the obstruction and along the channel.

The point at which the liquid film is completely prevented from falling downwards in the channel and is fully entrained by the gas phase outside the test section, is called the "zero penetration point".

In presenting the experimental results, it is usual to introduce the superficial velocity, J, defined as the volumetric flow rate of the phase considered divided by the total flow area. The free flow area offered by the obstruction was used for the evaluation of J.

Experimental data

The experimental results are presented in figures 2 and 3. In figure 2 the liquid flow rate collected at the bottom of the test section (i.e. not entrained by the gas), expressed as the delivered superficial velocity, $J_{L,d}$, is plotted vs the gas superficial velocity, J_G. It must be considered that because of the low liquid mass flow rates involved, it is possible to neglect the liquid film thickness in comparison with the obstruction diameter; therefore J_G represents, to a good approximation, the actual average gas velocity in the obstruction.

In the graphs of figure 2 the experimental results are grouped according to the obstruction flow diameter D_0. In figure 3 the delivered liquid mass flow rate is plotted vs J_G, and the experimental results are grouped according to the inlet water mass flow rate.

Looking at the experimental data, it is evident that reducing the penetration ratio, the zero penetration gas velocity decreases, ranging from 6 m/s at $D_0 = 12$ mm to about 12 m/s at $D_0 = 20$ mm (free channel diameter). A similar and even clearer trend is evident concerning the gas velocity at the onset of flooding, which ranges from 1–2 m/s at $D_0 = 12$ mm to 6–8 m/s at $D_0 = 20$ mm.

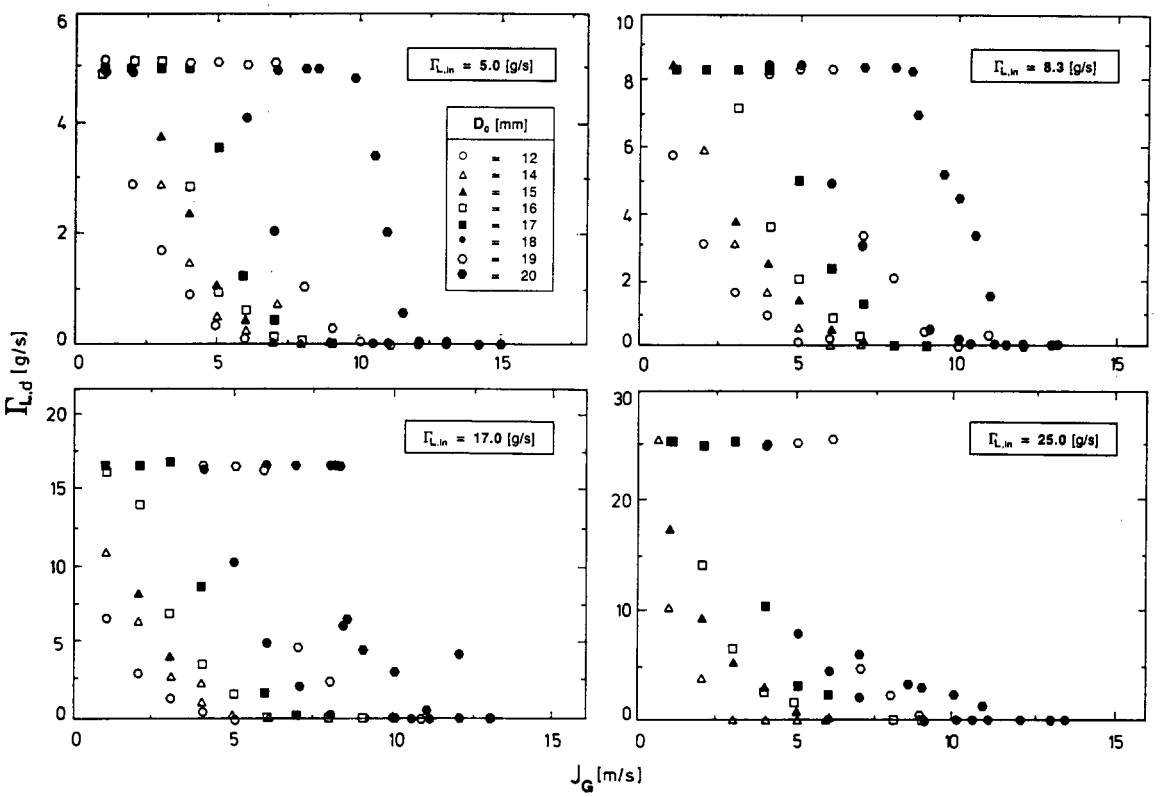

Figure 3. Experimental results: delivered liquid mass flow rate vs gas superficial velocity.

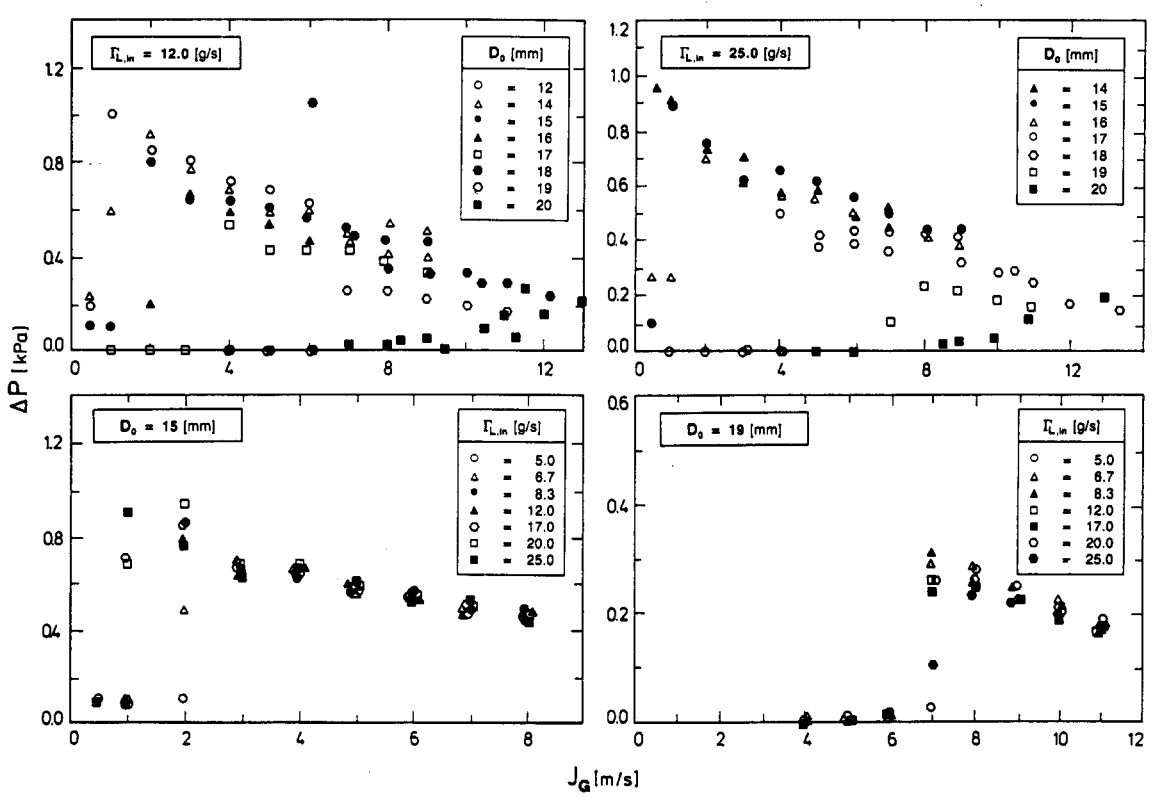

Figure 4. Pressure drop measurements across the obstruction vs gas superficial velocity.

For the same inlet water mass flow rate, a reduction in the obstruction flow diameter leads to an increase in the liquid film thickness. According to Wallis (1969) and Richter (1981), the liquid film thickness, δ, is related to the channel diameter as follows:

$$\delta \propto \left(\frac{Q_L}{D}\right)^{2/3}, \qquad [1]$$

being Q_L the liquid volumetric flow rate. It would seem reasonable to suppose that, at the same countercurrent gas velocity, a thicker liquid film eases the formation of superficial instabilities (waves) and then advances, in terms of local gas velocity, J_G, the perturbation of the liquid falling film and its entrainment by the gas stream. This hypothesis is also supported by the evidence that, for the same obstruction flow diameter, the gas velocity at the onset of flooding decreases as the inlet water mass flow rate increases (figure 2).

In figure 4 the experimental results of the pressure drop across the obstruction vs the superficial gas velocity are reported. They are grouped according to the obstruction flow diameter and the inlet water mass flow rate. The onset of flooding is characterized, and then easily evidenced, by a quick and significant increase in the measured pressure drop (up to 5–6 times the value measured in the absence of flooding) across the test channel. Just after the onset of flooding, the pressure drop decreases as the gas velocity, and hence the liquid entrainment, increase.

The absolute value of the maximum pressure drop depends, intuitively, both on the obstruction flow diameter, D_o, and on the inlet water mass flow rate, $\Gamma_{L,in}$; pressure drop is an increasing function of $\Gamma_{L,in}$, whilst it decreases as D_o increases. The influence of the obstruction flow diameter, D_o, on the gas velocity at the onset of flooding, $J_{G,of}$, is reported in figure 5, where $J_{G,of}$ is plotted vs the perforation ratio, γ. In a similar way, figure 6 shows the gas velocity at the zero penetration point, $J_{G,zp}$, vs γ .

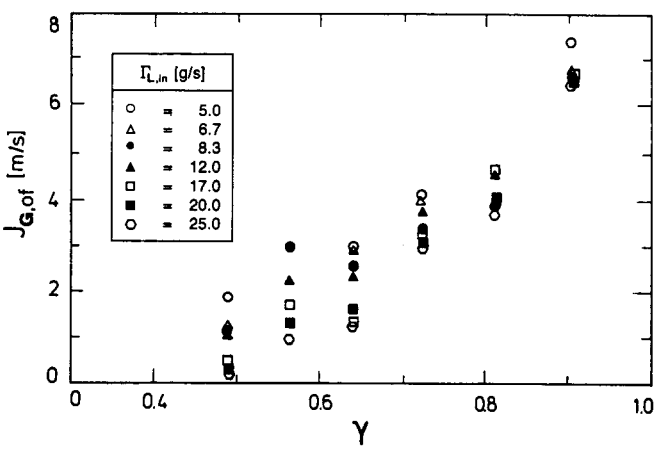

Figure 5. Superficial gas velocity at onset of flooding vs perforation ratio, γ.

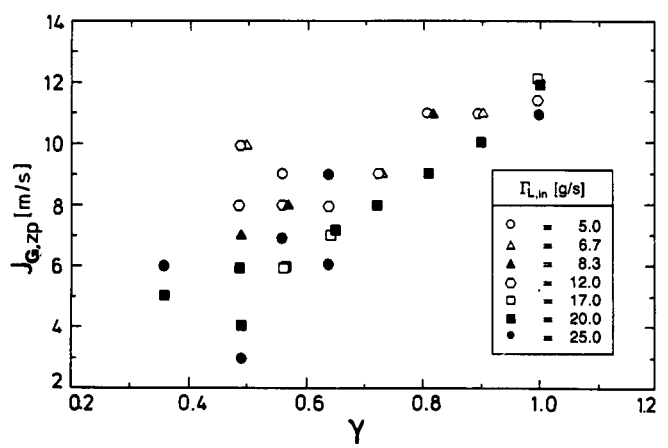

Figure 6. Superficial gas velocity at zero penetration vs perforation ratio, γ.

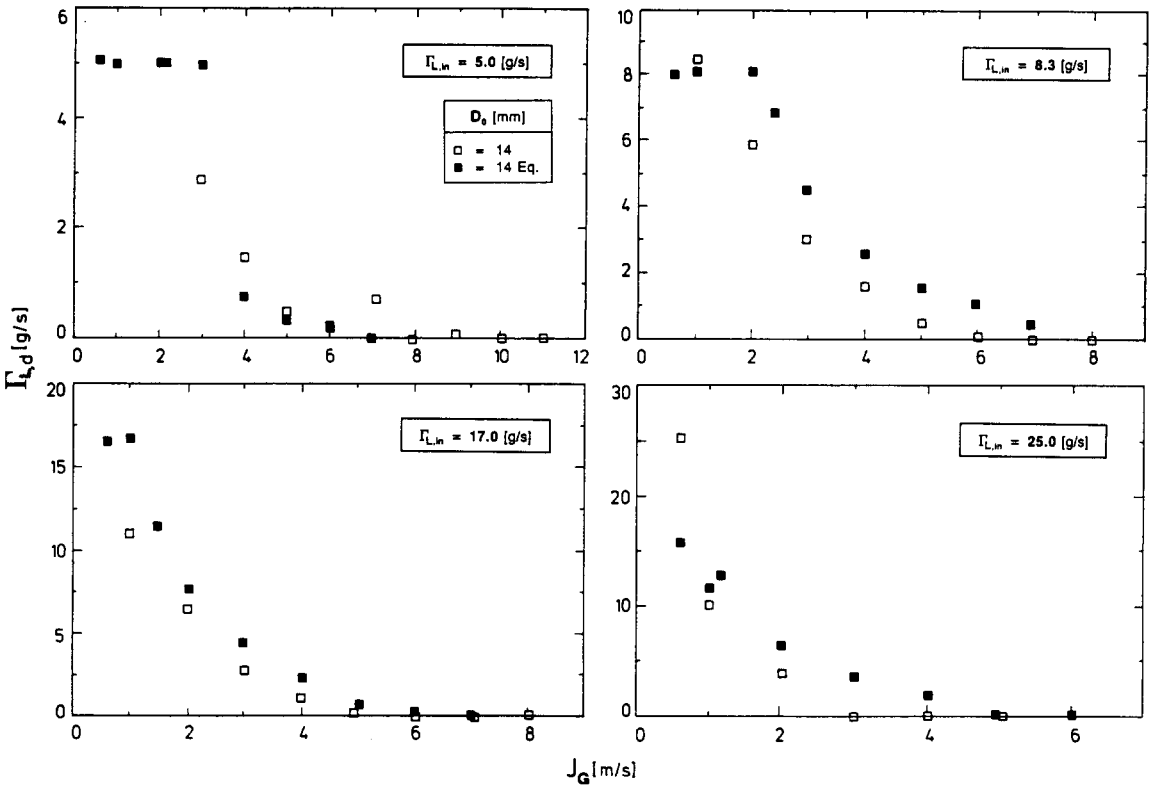

Figure 7. Comparison between single and multiple path flooding data.

Some of the performed tests refer to the analysis of the difference between flooding data in single and multiple short paths. For the obstruction diameter equal to 14 mm, a series of tests were carried out employing an obstruction with the same perforation ratio but with four 7 mm dia holes positioned symmetrically (multiple paths). The results are reported in figure 7, where the delivered mass flow rate is plotted vs J_G for the two geometries. For the two equivalent geometries used, it seems that the behavior, in terms of onset of flooding and zero penetration, is similar. More precisely, possible differences are within the experimental uncertainty of the measurements. However, considering the region between the onset of flooding and the zero penetration point, a systematically greater liquid entrainment in the simple geometry with respect to the complex one is evident.

It must be considered that, other conditions being equal, the liquid film thickness in the simple geometry (one hole) is thicker than in the complex geometry (four holes). In fact the cross section of each of the four holes is 1/4 of the total area offered by D_o, whilst the diameter is equal to $D_o/2$. In the case of equivalent geometries having the same flow cross section, the n holes have a diameter D_n given by

$$D_n = \frac{D}{\sqrt{n}}, \qquad [2]$$

where D is the diameter of the simple geometry. Therefore in the present case, with $n = 4$, indicating by δ_s and δ_c the liquid film thicknesses in the simple and complex geometry, respectively, and using [1], we have

$$\delta_s = 1.6\,\delta_c. \qquad [3]$$

Thus, according to the conclusions drawn in the first part of this section, the greater liquid entrainment in the simple geometry could be justified by the thicker liquid film, other conditions being equal.

4. DATA ANALYSIS

The first approach in the data analysis was the attempt to predict the experimental results with correlations available in the literature. Among the several correlations tested (Wallis 1961; Richter 1981; Dukler & Smith 1979; Chung *et al.* 1980; Pushkina & Sorokin 1969), only those proposed by Wallis (1961) and Dukler & Smith (1979) (essentially a modification of the Wallis correlation) gave an acceptable prediction of the experimental results.

The Wallis correlation is the most widely known and employed one for flooding data prediction, and has the form

$$J_G^{*1/2} + mJ_L^{*1/2} = C, \qquad [4]$$

where J_k^* for the k-phase is given by

$$J_k^* = J_k \left\{ \frac{\rho_k}{[gD(\rho_L - \rho_G)]} \right\}^{\frac{1}{2}}. \qquad [5]$$

In the case of air–water countercurrent flow, m can be assumed equal to 1. In fact (Bergles *et al.* 1981), m can be related to the dimensionless number

$$G = \left[\frac{\rho_L g D^3 (\rho_L - \rho_G)}{\mu_L^2} \right]^{\frac{1}{2}}, \qquad [6]$$

which represents the ratio between the gravitational and viscous forces. Generally, $m = 1$ for $G > 100$. In the present case, G ranges between 4000 ($D_o = 12$ mm) and 8500 ($D_o = 20$ mm, free channel condition).

As far as the constant C is concerned, it depends on inlet and outlet conditions, but Wallis (1961) suggested employing

$$0.725 \leqslant C \leqslant 0.875. \qquad [7]$$

Other researchers propose a value of C greater than those proposed by Wallis (1961): Dukler & Smith (1979) propose $C = 0.88$, whilst Hewitt & Wallis (1963) propose $C = 1 (J_L^* < 0.3)$.

Other tested correlations, based either on an empirical or on a theoretical approach, have not been reported in this paper because of their poor agreement with the experimental data.

Among the correlations available in the literature, the one proposed by Bankoff *et al.* (1981) is of some interest, since it was developed for perforated plates. Bankoff *et al.* suggested an interpolation scaling parameter H^* between the J^*—[5]—and K parameters. The parameter K, known as the Kutateladze number, for phase k, is defined as

$$K_k = J_k \left\{ \frac{\rho_k^2}{[g\sigma(\rho_L - \rho_G)]} \right\}^{\frac{1}{4}}. \qquad [8]$$

The interpolation scaling parameter H^* is defined by the following relation:

$$H_k^* = J_k \left[\frac{\rho_k}{gw(\rho_L - \rho_G)} \right]^{\frac{1}{2}}, \qquad [9]$$

where the interpolative length scale w is

$$w = D^{1-\beta} \left[\frac{\sigma}{g(\rho_L - \rho_G)} \right]^{\beta/2}, \qquad 0 \leqslant \beta \leqslant 1; \qquad [10]$$

and where the empirical exponent β is correlated for data related to the particular geometry of interest.

Bankoff *et al.* (1981) suggested the following trial function:

$$\beta = \tanh(\gamma K_c D_o), \qquad [11]$$

where the critical wavenumber $K_c = 2\pi / t_o$, corresponds to the maximum wavelength which can be sustained on an interface of length t_o, in this case the disk thickness; and γ is the perforation ratio. Equation [11] implies that H_k^* approaches J_k^* for small diameters ($\beta \to 0$), and K_k for large diameters ($\beta \to 1$).

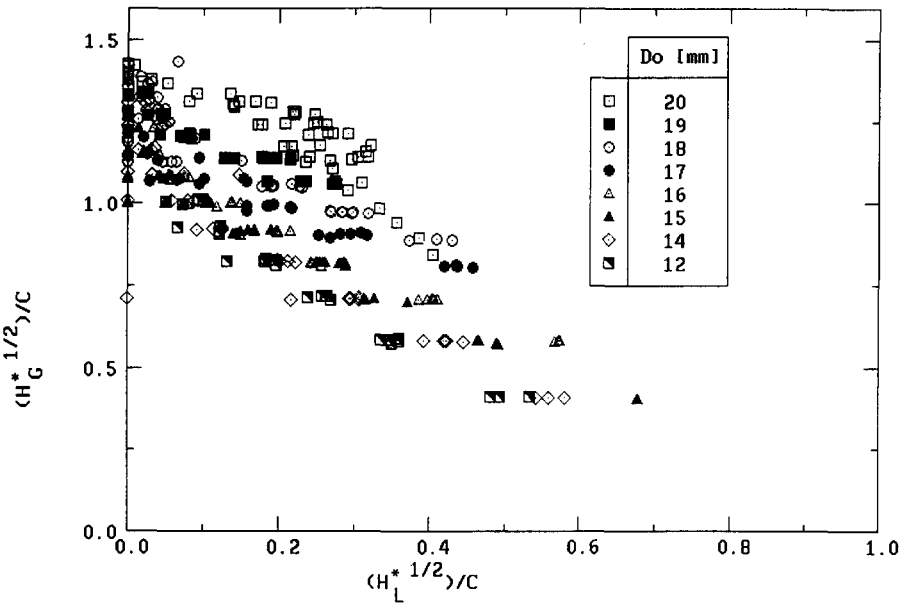

Figure 8. Comparison between the experimental data and predictions by the Bankoff *et al.* (1981) correlation.

In our experiment, because of the low value of t_o (1/10 of D_o, i.e. $t_o \leqslant 2$ mm) in comparison with Bankoff's data ($t_o = 20$ mm), we always gave $\beta = 1$. So, practically, the correlation proposed by Bankoff *et al.* (1981),

$$H_G^{*1/2} + H_L^{*1/2} = C, \qquad [12]$$

becomes the Kutateladze correlation (Bankoff & Lee 1983). According to Richter (1981), the Wallis correlation [4] is consistent with data for pipe sizes up to 50 mm dia, whilst the Kutateladze correlation applies for pipe sizes >150 mm dia. Consequently, [12] seems to be bound to fail. Anyhow, the comparison between the experimental data and the predictions obtained using the Bankoff correlation [12] is shown in figure 8. The agreement is poor, as expected.

The predictions obtained using the Wallis (1961), Dukler & Smith (1979) and Hewitt & Wallis (1963) correlations are compared with the experimental data in figure 9, grouped according to the obstruction flow diameter, D_o. The agreement between the Wallis correlation and the experimental data is not satisfactory when an obstruction is present in the channel, but the comparison enables us to formulate the following conclusions:

1. The Wallis correlation, according to the suggestions by Hewitt & Wallis (1963) concerning the constant C (C = 1), represents to a good accuracy and precision the present experimental data for $D_o = 20$ mm (free channel).
2. Figure 9 shows that decreasing D_o, the experimental points tend to lie along a straight line parallel to that corresponding to [4] with C = 1, shifting towards a region of the Wallis plane characterized by decreasing values of the constant C.

In conclusion, the Wallis correlation would seem to be able to predict the experimental data with obstructions in the flow channel, if we chose, for each value of D_o, a suitable value of the constant C. On the other hand, it is necessary to say that C, according to Wallis (1961), is a function of the water inlet conditions and the geometry. As the flooding occurs just in the obstructing flow cross section, where the gas velocity reaches its maximum value, it would seem reasonable to link the constant C to the obstruction diameter, or better, to γ.

In figure 10, values of C determined experimentally are plotted vs γ. From a best-fit procedure we found a relationship of the type

$$C = C_o \gamma^{0.35}, \qquad [13]$$

with $C_o = 1$ (Hewitt & Wallis constant).

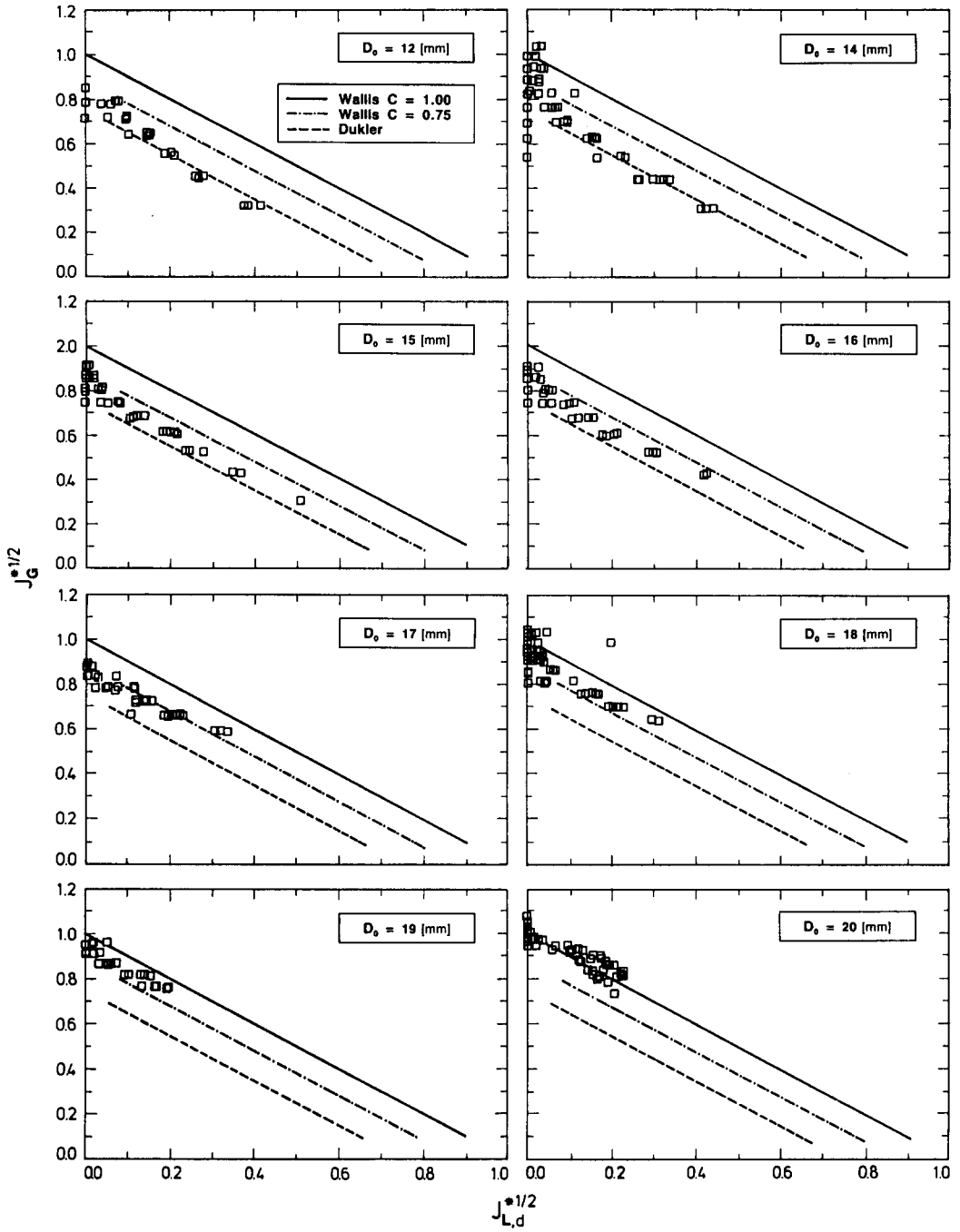

Figure 9. Comparison between the experimental data and predictions by the Wallis (1961), Dukler & Smith (1979) and Hewitt & Wallis (1963) correlations.

The predictions obtained using [4] and [13] are compared with the experimental results in figure 11. The agreement turns out to be satisfactory for all the obstruction diameters investigated.

Analyzing the comparison in more detail, the agreement is very good as regards the onset of flooding and the partial delivery region of increasing gas velocity, whilst poorer agreement (however, within a $\pm 20\%$ confidence level) is shown in the prediction of zero penetration conditions. This limit was also shown by the original Wallis correlation ($C_o = 1$) in predicting $D_o = 20$ mm data. It must be said that these experimental points are affected by a high experimental uncertainty.

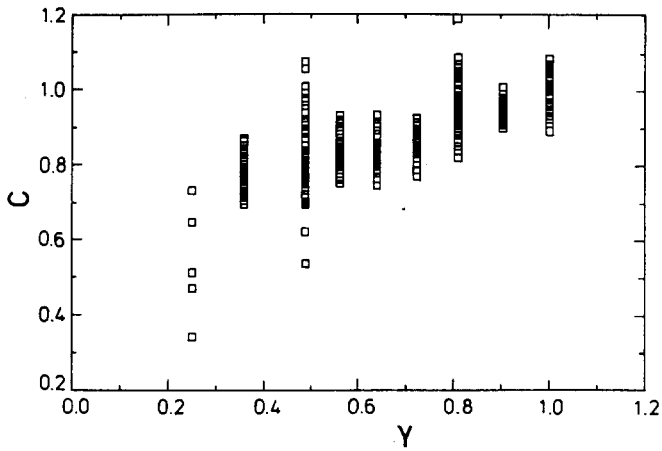

Figure 10. Experimental values of the constant C in the Wallis (1961) correlation.

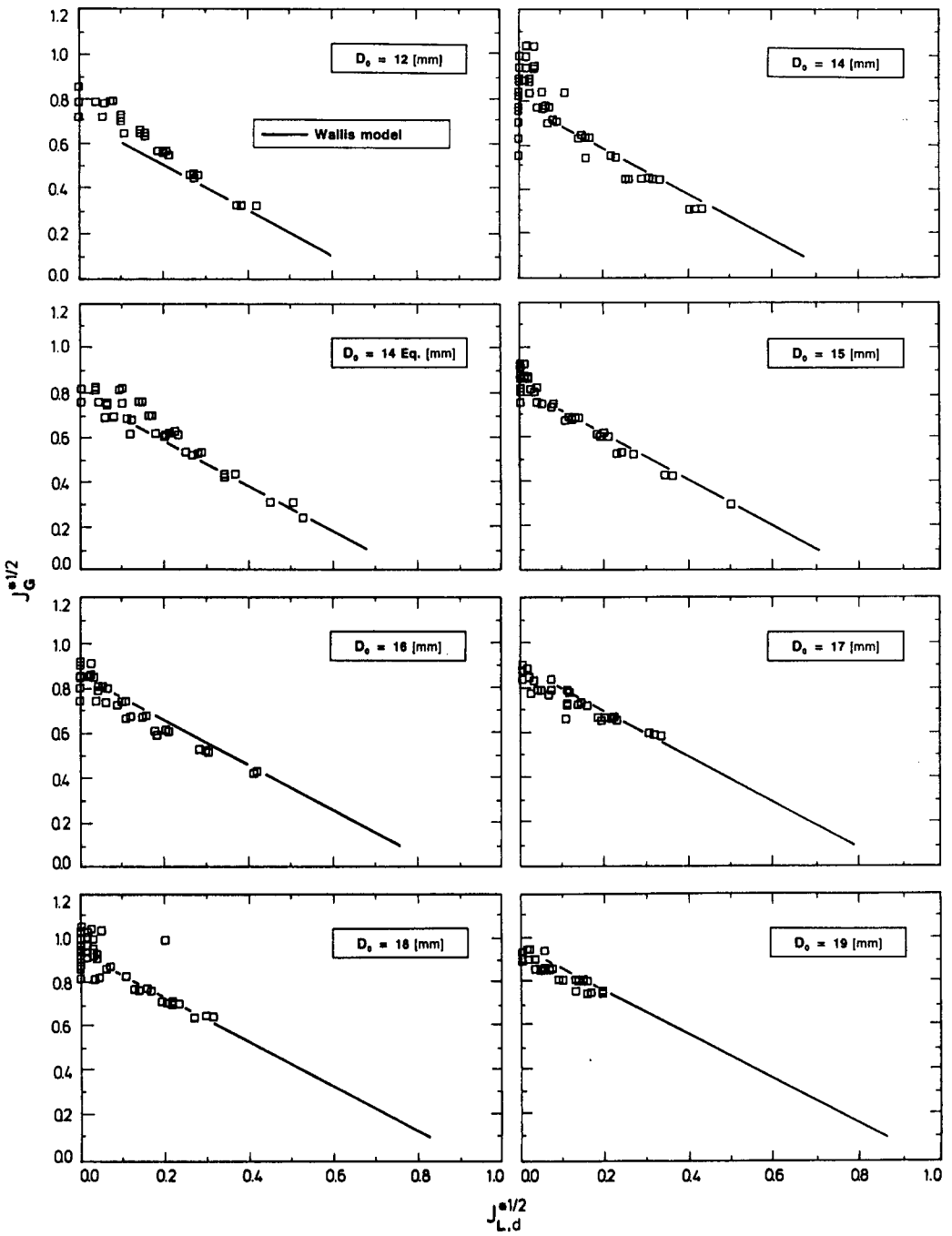

Figure 11. Comparison between the experimental data and predictions obtained using the modified Wallis correlation.

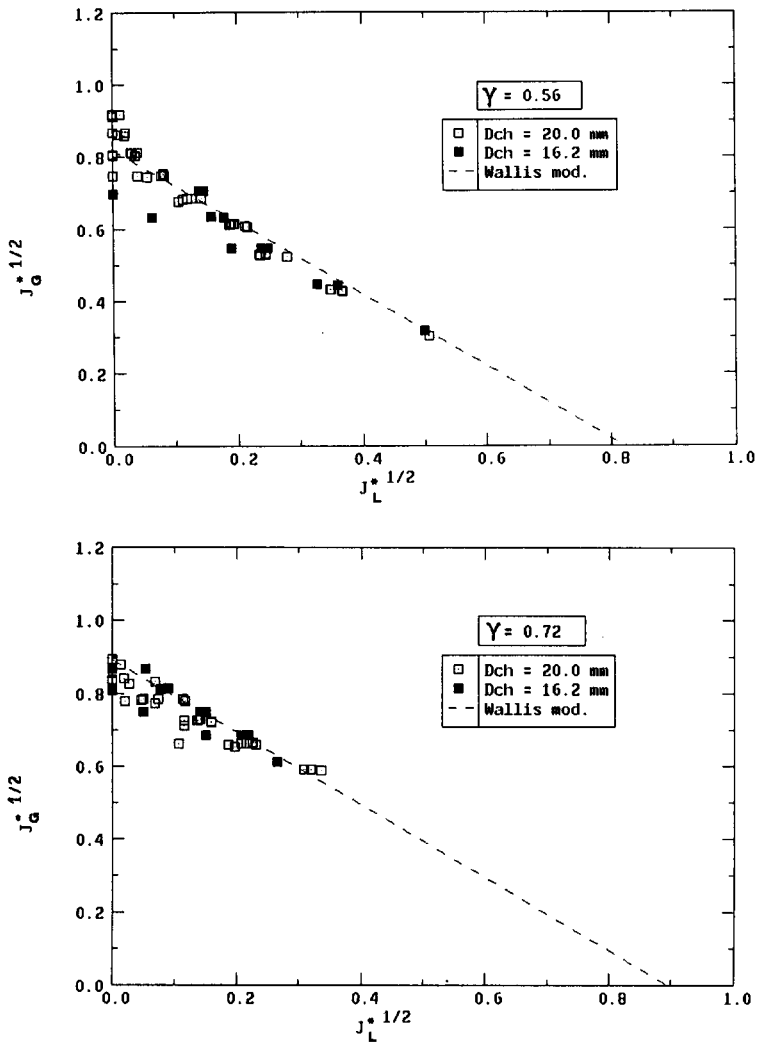

Figure 12. Comparison between 20 and 16.2 mm dia channel data; predictions by the modified Wallis correlation.

In addition to the good agreement with the experimental data, the Wallis correlation (represented by the straight line) has the great advantage of being very simple. Indeed, more complex correlations and theoretical models have shown a clear inadequacy in predicting experimental data different from those from which they were developed.

In order to check the validity of [13] in a different geometry, we performed experiments with the same values of γ (0.56 and 0.72) but with a 16.2 mm dia channel (L/D was the same). The predictions of these data obtained using [4] and [13] are reported in figure 12. The agreement with the experimental data is quite good and the comparison between the 20.0 and 16.2 mm data does not show any systematic difference.

Concerning the zero penetration point data, from [4] and [13], we have

$$J^*_{G.zp} = C_o^2 \gamma^{0.7}. \qquad [14]$$

Predictions obtained using [14] are compared with the experimental data in figure 13 where $J^*_{G.zp}$ is plotted vs the dimensionless diameter, D^*, defined as follows:

$$D^* = D\left[\frac{g(\rho_L - \rho_G)}{\sigma}\right]^{\frac{1}{2}}. \qquad [15]$$

The agreement is satisfactory, whilst the comparison with the predictions obtained using the Bankoff *et al.* (1981) and Richter (1981) correlations is decisively poor.

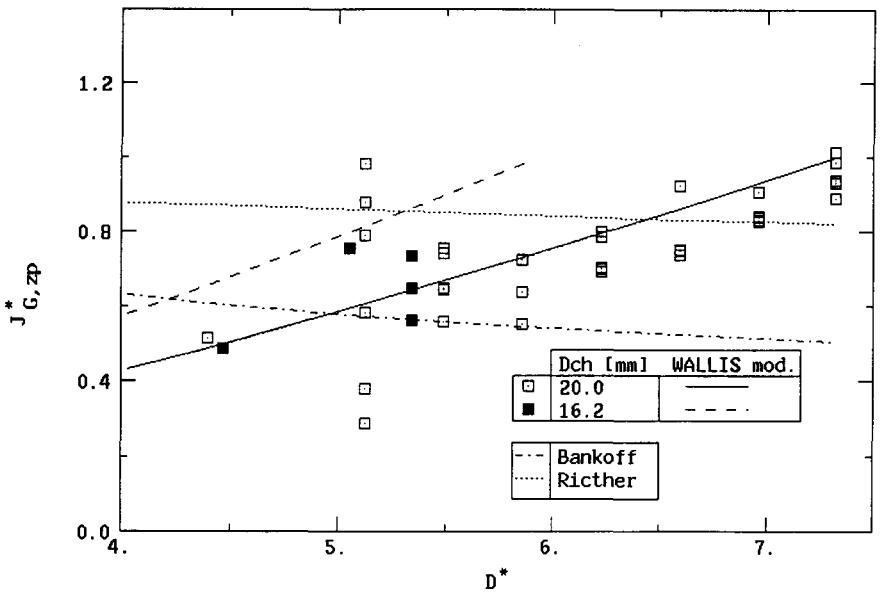

Figure 13. Zero penetration point: experimental data and predictions.

5. CONCLUDING REMARKS

An experimental investigation of the flooding phenomenon was performed, with particular reference to the influence of obstructions placed inside the flow channel. Such obstructions were characterized by a circular cross section, and the free flow area ranged between 35 and 100% of the test channel cross section ($D_0 = 20$ mm).

It is shown how the obstruction advances the flooding phenomenon, other conditions being equal. A marginal influence is shown by the shape of the flow obstruction, at least for the obstructions tested.

A slightly modified Wallis correlation enables good prediction of the experimental data obtained with two different channel diameters.

REFERENCES

BANKOFF, S. G. & LEE, S. C. 1983 A comparison of flooding models for air–water and steam–water flow. In *Advances in Two-Phase Flow and Heat Transfer*; *NATO ASI Series E*, No. 64 (Edited by KAKAC, S. & ISHII, M.), pp. 695–728. Hemisphere, Washington, D.C.

BANKOFF, S. G. & LEE, S. C. 1986 A critical review of the flooding literature. In *Multiphase Science and Technology*, Vol. 2 (Edited by HEWITT, G. F., DELHAYE, J. M. & ZUBER, N.), pp. 95–180. Hemisphere, Washington, D.C.

BANKOFF, S. G., TANKIN, R. S., YUEN, M. C. & HSIEH, C. L. 1981 Countercurrent flow of air/water and steam/water through a horizontal perforated plate. *Int. J. Heat Mass Transfer* **24,** 1381–1395.

BERGLES, A. E., COLLIER, J. G., DELHAYE, J. M., HEWITT, G. F. & MAYINGER, F. 1981 *Two-phase Flow and Heat Transfer in the Power and Process Industries.* Hemisphere, Washington, D.C.

CHUNG, S. K., LIU, L. P. & TIEN, C. L. 1980 Flooding in two-phase countercurrent flows—experimental investigation. *Physicochem. Hydrodynam.* **1,** 209–220.

DUKLER, A. E. & SMITH, L. 1979 Two-phase interactions in countercurrent flow: studies of the flooding mechanism. Report NUREG/CR-0617, NRC, Washington, D.C.

HEWITT, G. F. & WALLIS, G. B. 1963 Flooding and associated phenomena in falling film flow in a vertical tube. Report AERE-R4022, UKAEA, Harwell, Oxon.

PUSHKINA, O. L. & SOROKIN, Y. L. 1969 Breakdown of liquid film motion in vertical tubes. *Heat Transfer Sov. Res.* **1**, 56–64.

RICHTER, H. J. 1981 Flooding in tubes and annuli. *Int. J. Multiphase Flow* **7**, 647–658.

WALLIS, G. B. 1961 Flooding velocities for air and water in vertical tubes. Report AAEW-R123, UKAEA, Harwell, Oxon.

WALLIS, G. B. 1969 *One-dimensional Two-phase Flow*. McGraw-Hill, New York.